Chemical Engineering Journal 429 (2022) 132304

Contents lists available at ScienceDirect

Chemical Engineering Journal

journal homepage: www.elsevier.com/locate/cej

Fabrication of MIL-101-polydimethylsiloxane composites for environmental toluene abatement from humid air

Luqman Hakim Mohd Azmi [a,b], Pavani Cherukupally [a], Elwin Hunter-Sellars [a], Bradley P. Ladewig [a,c], Daryl R. Williams [a,*]

[a] Department of Chemical Engineering, Imperial College London, South Kensington Campus, Exhibition Road, London, SW7 2AZ, UK
[b] Grantham Institute – Climate Change and the Environment, Imperial College London, South Kensington Campus, Exhibition Road, London, SW7 2AZ, UK
[c] Institute of Micro Process Engineering (IMVT), Karlsruhe Institute of Technology, Hermann-von-Helmholtz-Platz 1, 76344 Eggenstein-Leopoldshafen, Germany

ARTICLE INFO

Keywords:
Adsorption
Hydrophobic
Metal–organic frameworks (MOFs)
polydimethylsiloxane (PDMS)
Toluene
volatile organic compounds (VOCs)

ABSTRACT

Competition for adsorption sites between atmospheric moisture and volatile organic compounds (VOCs) can significantly impact the VOC removal performance of novel metal–organic framework adsorbent such as MIL-101. MIL-101 has high surface area and high porosity, but its inherent hydrophilicity hinders selectivity for hydrophobic organic species in the presence of atmospheric moisture. In this study, a vapor phase deposition of polydimethylsiloxane (PDMS) was used to create more hydrophobic MIL-101 composites. The external hydrophobicity of the composites was evaluated through water contact angle measurements whereas the internal hydrophobicity was assessed using a vapor-sorption based hydrophobicity index. After an optimized vapor deposition time of 0.25 hr employing a low molecular weight PDMS, a MIL-101 composite with enhanced internal hydrophobicity and intact porosity was fabricated. The composite's efficacy for VOC capture was investigated through toluene-water vapor co-adsorption experiments which involved vapor adsorption at 40% RH and at two toluene concentrations: 0.5% P/P_0 and 10% P/P_0. At 0.5% toluene P/P_0, the new composite exhibited almost 60% higher adsorption capacity and 34% higher overall capture rate relative to pristine MIL-101 due to the presence of a hydrophobic PDMS layer which delayed the onset of water condensation in the mesopores. At 10% toluene P/P_0, the new composite's overall toluene uptake was 2.8 times higher than activated carbon, but slightly lower than pristine MIL-101. This new composite also showed excellent structural stability and adsorption performance after 10 sorption/desorption cycles. The superior performance of the MIL-101-PDMS composite could be utilized to selectively remove toluene from real world humidities and VOC concentrations.

1. Introduction

Volatile organic compounds (VOCs) released by various indoor and outdoor processes, such as automobile emissions, chemical production processes and consumer product usage can all severely contaminate air quality [1–3]. There is an urgent need for novel materials that can adsorb VOCs in real world conditions, thus minimizing their negative impacts on environment [2,4] and public health [5,6]. An especially significant challenge is to minimize the loss of VOC capture performance by adsorbents because of preferential moisture adsorption.

VOC removal from contaminated air using porous adsorbents is an established method of separation [7,8]. Carbon-based adsorbents which are in common usage are low cost, have high porosity, and good chemical stability, rendering them ubiquitous for use in air purification devices. However, their amorphous, heterogeneous chemical structures make targeted removal of specific hydrocarbon species challenging [9]. Recently, metal–organic frameworks (MOFs) emerged as a new class of adsorbents for targeted capture, storage, and release of organic vapours in a controlled fashion. Furthermore, the extensive metal-linker possibilities endow them with an orderly pore structure, high surface area, and excellent selectivity for VOC removal [10,11]. The practical usage of MOFs for removing VOCs is nonetheless limited by their adsorption competition with omnipresent moisture in the environment, which is especially problematic for polar or hydrophilic MOF materials.

An efficient adsorbent should exhibit high selectivity, high uptake capacity, and fast kinetics for targeted removal of a specific VOC species. In the atmosphere, water vapor exists at 10000 times or higher concentrations than many VOC species concentrations. Consequently,

* Corresponding author.
E-mail address: d.r.williams@imperial.ac.uk (D.R. Williams).

https://doi.org/10.1016/j.cej.2021.132304
Received 29 June 2021; Received in revised form 1 September 2021; Accepted 2 September 2021
Available online 8 September 2021

relative to VOCs, the water molecules get favourably adsorbed onto the adsorbents at these higher concentrations, resulting in poor VOC uptake. The maximum uptake capacity and kinetics of VOCs adsorption depend on several key factors such as available surface area, surface chemical groups, pore volume, and pore size of the adsorbent [12]. Therefore, MOFs could be designed using these criteria to adsorb toxic aromatic hydrocarbons from ambient air, while rejecting water molecules [9,13].

Among the currently available MOFs, MIL-101 is frequently studied for VOC capture [14–17] as it has high surface area and pore volume, tuneable surface properties, and excellent hydrothermal stability [18]. However, the natural hydrophilicity of MIL-101 [19,20] results in low selectivity for common hydrophobic VOCs, especially in humid environments. Typically, a MOF's hydrophobicity can be improved using three surface modification strategies: ligand functionalization with hydrophobic moieties [21,22], in-situ hydrophobization [23–25], and post-synthetic modification [26,27]. Of these methods, post-synthetic modification via coatings is preferred because of its low cost, controllable, simple and scalable fabrication process [13,26]. Therefore, gas phase coating techniques, such as polymer vapor deposition could be a suitable approach to enhance MIL-101′s selectivity and kinetics for VOCs adsorption from air [10].

Polydimethylsiloxane (PDMS) is a common hydrophobic, silicon-based polymer that prevents liquids, but permits gases to diffuse through the surfaces [28]. With its excellent hydrophobicity, gas phase selectivity, and low cost, PDMS can be considered as a promising coating material for enhancing the hydrophobicity of MIL-101. To date, research efforts have been focused on synthesizing MOF-PDMS composites, though not for VOC capture applications [29–33]. Encouraging data from competitive benzene-moisture adsorption experiments has been reported for activated carbon (AC)-PDMS composites [34] although specific water sorption isotherms were not reported, and the authors used an unrealistic benzene concentration of >1400 ppm. The US Occupational Safety and Health Administration (OSHA) has set a permissible exposure limit of 1 ppm for benzene in the workplace during an 8-hour workday within a 40-hour workweek, and the UK has the same exposure limit [35].

Given MIL-101′s high porosity and surface area, combined with the hydrophobicity of the PDMS, MIL-101-PDMS composites could potentially exhibit high selectivity and uptake of VOCs. In this work, a series of PDMS-coated MIL-101 materials for VOC capture were prepared by tuning the PDMS coating timescale and the molecular weights, followed by an evaluation of their effectiveness for competitive co-adsorption of toluene and water vapor. Toluene co-adsorption studies were performed at 0.5% P/P_0 (188 ppm) and 10% P/P_0 (3750 ppm) with 40% relative humidity (RH) at 25 °C. The 188 ppm is in the mid-range of the environmental concentration for human exposure; the OSHA Permissible Exposure Limits are 200 ppm while the National Institute for Occupational Safety and Health (NIOSH) Recommended Exposure Limit (REL) is 100 ppm [36]. On the other hand, the 3750 ppm is meant to represent an industrial solvent-recovery scenario. All tests were conducted alongside pristine MIL-101 as well as AC for a more comparative understanding.

2. Material and methods

2.1. Material

Chromium (VI) nitrate nonahydrate (98%), terephthalic acid (99%), PDMS-Sigma (dynamic viscosity, $\mu = 10$ cST), were supplied by Sigma-Aldrich. Glacial acetic acid (100%) was purchased from VWR and toluene (ACS, 99.5%) was purchased from Alfa Aesar. Silicone elastomer kit SYLGARD^{TM} 184 was ordered from Dow Chemical Company. This 2-part kit contains PDMS and a curing agent, but only the PDMS was used, herein denoted as PDMS-Dow ($\mu = 3500$ cST). The reference adsorbent is a commercial granular activated charcoal (AC) F400 procured from Chemviron Carbon.

2.2. Synthesis of MIL-101

Hydrofluoric acid-free MIL-101 was synthesized by preparing equimolar quantities of chromium (VI) nitrate nonahydrate (5 mmol, 2 g), terephthalic acid (0.83 g) and acetic acid (0.29 mL) to be dissolved in 25 mL of water [37]. The mixture was sealed in a Teflon-lined reactor and heated in an oven at 220 °C for 8 hrs. The resultant green crystals were centrifuged and thoroughly rinsed with water (20 mL × 2) and ethanol (20 mL × 1) to remove unreacted terephthalic acid from the product. The suspension was finally dried overnight in a vacuum oven at 120 °C to obtain dehydrated MIL-101 product.

2.3. PDMS coating method

50 – 100 mg of activated MIL-101 was spread in a small glass petri dish to form a thin powder layer. The dish containing the substrate was placed inside a larger dish filled with liquid PDMS. Both dishes were covered with aluminium foil and then heated in an oven. The dish containing PDMS-Dow was heated at 235 °C while PDMS-Sigma at 180 °C for a series of specific coating times. After the coating time completed, the sample was left to cool, yielding a range of coated MIL-101 samples designated as MIL-PDMS-XXX-T. The suffix XXX describes the PDMS source and T represents the time spent in the oven (hr). Different oven temperatures were used depending on the PDMS boiling points to ensure polymer volatility [38]. Fig. S1 in the Supplementary Information shows the gas-phase deposition experimental setup in more detail.

2.4. Material characterization

Powder x-ray diffraction (PXRD) spectra were recorded on X'Pert PRO PANalytical diffractometer using Cu Kα radiation (40 kV, 20 mA) within a scattering range (2θ) from 5° to 30°. The theoretical PXRD spectra of MIL-101 were derived from the Cambridge Crystallographic Data Centre (CCDC) code OCUNAC. FTIR spectra were measured with Cary 630 spectrometer (Agilent, USA). Thermal stability of the coated samples was examined using a thermogravimetric analyser (TGA) instrument Netzsch STA 449 *F5 Jupiter*® from 30° to 900 °C under flowing air (40 mL/min) at a heating rate of 20 K/min. Nitrogen (N_2) adsorption–desorption measurements were conducted with 3Flex Micromeritics analyser at 77 K from partial pressures (P/P_0) of 0 to 0.99. Prior to testing, the samples were degassed overnight in vacuo at 150 °C. Brunauer Emmett Teller (BET) method was used to calculate the specific surface area of the adsorbents. External surface area and micropore volume (V_{micro}) were estimated from the respective adsorbent's t-plot. Total pore volume (V_{total}) and pore size distribution were estimated according to Tarazona non-local density functional theory (NLDFT) N_2 model by assuming a cylindrical pore geometry. X-ray fluorescence (XRF) measurements for the samples were performed on PANalytical Epsilon 3XLE XRF spectrometer. SEM images were acquired using Zeiss Leo Gemini 1525 operated at 5 kV. A Krüss drop shape analyser was used to measure the samples' static water contact angle at ambient temperature.

2.5. Single-solvent adsorption measurements

The solvent adsorption experiments were performed at 25 °C with water and toluene in static mode using IGA-002 (Hiden Isochema, UK). Dynamic and competitive isotherms were obtained using DVS Resolution (Surface Measurement Systems, UK). Toluene was chosen as a model hydrophobic VOC molecule. It is a relatively common environmental VOC with exposure limits in the 100 to 200 ppm range [36] and was tested at 188 ppm in the current study. Descriptions on the humid toluene adsorption experimental methodology can be found in Fig. S2.

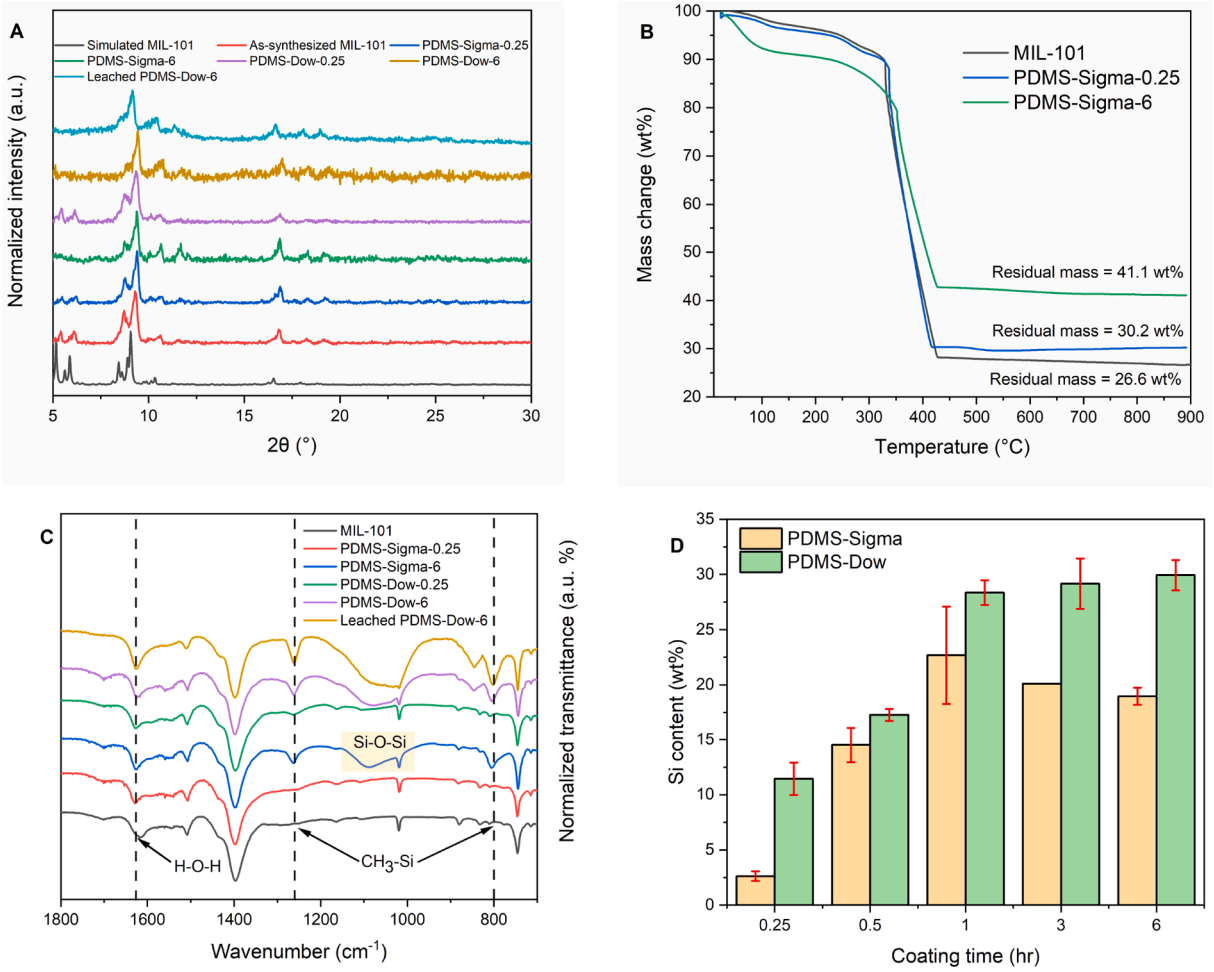

Fig. 1. (A) PXRD spectra of PDMS-coated samples. (B) Thermal decomposition profiles of the composites in air atmosphere (40 mL/min). (C) FTIR spectra of the composites. (D) Elemental Si wt% quantification by XRF.

2.6. Hydrophobicity index

An effective VOC adsorbent requires hydrophobicity on both internal pore surfaces as well as external surfaces for optimal organic molecule adsorption [13]. However, contact angle measurements only determine the hydrophobicity for the outer surface, but not for the surface of the internal pores. Furthermore, contact angle measurements do not consider factors specific to adsorption performance including differences in size, volume, and shape of the pores. To address this gap, the internal adsorbent hydrophobicity is usually evaluated through water and other vapour/gas adsorption isotherms. A recently proposed hydrophobicity index (HI) was used in this study as a comprehensive and quantitative descriptor of pore hydrophobicity. In general, hydrophobicity indexes take into account a material's adsorption capacity ratio for a hydrophobic molecule such as toluene [39] or cyclohexane [40] relative to water, either obtained from separate single [39] or dual component adsorption experiments [41]. Alternatively, other hydrophobicity indexes can also be estimated through pore volume measurement from N_2 adsorption and volume of desorbed water from TGA analysis [42]. A representative comparison of the reported hydrophobicity indexes values can only be achieved if the mode of the hydrophobicity index experiment is clearly specified, either conducted in dynamic (simultaneous exposure of competing species) or static (separate exposure). Eq. (1) shows the preferred HI calculation formula used in this study [43] which allows a humidity dependent metric to be determined (static mode):

$$HI_{static}(x) = \frac{Q_{toluene-0.05}}{Q_{water-x}} \quad (1)$$

where $HI_{static}(x)$ (mol/mol) is the material's molar hydrophobicity index calculated using the quantity of toluene adsorbed at 5% toluene P/P_0 ($Q_{toluene\text{-}0.05}$, mol/g) as a function of adsorbed water quantity ($Q_{water\text{-}x}$, mol/g) at different water humidity expressed as P/P_0 (x).

2.7. Competitive adsorption experiments

To mimic real-world conditions, the adsorbent samples were pre-exposed in separate experiments at 0.5% P/P_0 and at 10% P/P_0 simultaneously with 40% RH of water vapor at 25 °C. It is acknowledged that factors such as geographical, seasonal, and building environments can influence the average building humidity levels, however, 40% RH can be reasonably considered as a typical daily average indoor value and is the focus for the current study. At a high humidity condition (80% RH), the samples showed negligible toluene uptake because water adsorption process overwhelmed any measurable toluene adsorption. So, the performance of all adsorbents was evaluated at 40% RH and two separate toluene concentrations of 0.5% P/P_0 and at 10% P/P_0, representing a mid-range environmental VOC concentration of interest, and concentration from an industrial solvent separation/recovery process, respectively.

Table 1
Surface area, pore volume and water contact angles for all MIL-101 samples and AC.

Sample	BET surface area (m^2/g)	External surface area (m^2/g)	V_{total} (cm^3/g)	V_{micro} (cm^3/g)	V_{micro}/V_{total}	Water contact angle (°)
MIL-101	2607 ± 56	227	1.705	1.127	0.661	0
MIL-PDMS-Sigma-0.25*	2865 ± 76	287	1.797	1.231	0.685	0
MIL-PDMS-Sigma-6	1192 ± 7	145	1.006	0.477	0.474	131 ± 1
MIL-PDMS-Dow-0.25*	2398 ± 35	277	1.488	0.979	0.658	0
MIL-PDMS-Dow-6	656 ± 1	115	0.672	0.237	0.353	133 ± 3
Activated carbon (AC)	1358 ± 2	242	0.805	0.470	0.584	120 ± 2†

* Higher values due to batch-to-batch variations in synthesis process.
† Taken from [45].

2.8. Moisture stability and adsorbent reusability tests

The materials were assessed for their short-term chemical stability at a high RH condition where other MOF adsorbents are known to be unstable. Starting with (A) a 40% RH background, the samples were first equilibrated with 0.5% toluene P/P_0, then exposed to (B) 90% RH at 0% toluene P/P_0 for 24 hrs. Finally, they were tested at (C) 40% RH and 0.5% toluene P/P_0 again. The toluene uptake (A) before and (C) after the 90% RH exposure was reported as a metric for their hydro-stability. In the reusability experiment, also undertaken at 40% RH background, the samples were exposed to 10% toluene P/P_0 for 3 hrs followed by 1 hr of desorption and repeated for 10 experimental cycles. All experiments were conducted at 25 °C.

3. Results and discussion

3.1. Solid state characterization

Fig. 1A shows the PXRD spectra of the samples. The identical 2θ peaks at 8.7°, 9.3°, 10.6° and 16.9° exhibited by all coated materials signify their intact crystallinity relative to the theoretical peaks of MIL-101. However, MIL-PDMS-Dow-6 exhibited slightly degraded peaks. The high coating temperature of 235 °C could be the reason for its crystallinity loss. The TGA plots in Fig. 1B compare the thermal decomposition of PDMS-Sigma samples to the pristine MIL-101 in an air atmosphere. The oxidative deposition atmosphere may have also accelerated the MOF degradation. Fig. S3 shows the SEM images for the studied samples. Irrespective of heating temperature, they display the typical octahedral morphology of MIL-101 crystals. The PDMS coating contents in MIL-PDMS-Sigma-0.25 and MIL-PDMS-Sigma-6 were measured as 0.14 wt % and 0.55 wt%, respectively. Details for the calculation methodology using Eq. S1 and further explanations of the TGA plots (Section S3) are given in the Supplementary Information.

The PDMS coating presence on MIL-101 was identified using FTIR spectroscopy. The FTIR spectra in Fig. 1C of all PDMS-coated samples display the characteristic vibration of Si—O—Si bonds [44]. The chemical stability or leaching of the coating was also studied with the findings described in Section S5. The XRF analysis in Fig. 1D illustrates the cumulative PDMS deposition for different coating time as represented by elemental Si wt%. Generally, the Si coating quantities for both PDMS types had plateaued at about 1 hr.

3.2. Porosity analysis

In a chemical vapour deposition (CVD) method, the coating time would directly influence the amount of coating deposited on the outer surface and in the pore surface of the MOFs. Therefore, the effect of PDMS exposure time to the MOF's pore volume was evaluated at 0.25 and 6 hrs. The complete (up to 0.99 N_2 P/P_0) and the low P/P_0 range (maximum of 0.1 N_2 P/P_0) N_2 adsorption and desorption isotherm plots are shown in Fig. S4 and S5 respectively. In Fig. S4, the MIL-PDMS-Dow-6 and MIL-PDMS-Sigma-6 both seem to have lost their mesoporosity, since there is no characteristic abrupt mesopore filling (after capillary condensation) at around 0.2 N_2 P/P_0. Instead, after this point, their adsorption isotherms became quite flat which supports their major loss of mesoporosity. Below 0.1 N_2 P/P_0 (Fig. S5), the first group (MIL-101, MIL-PDMS-Sigma-0.25, MIL-PDMS-Dow-0.25) showed higher microporous adsorption quantity than the second group (MIL-PDMS-Sigma-6, MIL-PDMS-Dow-6). The micropores for the adsorbents in the second group are likely to be severely blocked. Table 1 provides the details of the BET surface area and total pore volume measurements where it indicates that an extension from 0.25 hr to 6 hrs of coating reduced the V_{micro}/V_{total} ratio. This change is also visually identifiable from the adsorbents' pore size distribution plots (Fig. S6). For the second group, there is a significant drop in the micropore region which continues into the mesopore region.

For MIL-PDMS-Sigma, the total surface area and the pore volume were each 140% and 79% higher for 0.25 hr relative to 6 hrs coating. Whilst for MIL-PDMS-Dow, the total surface area and the pore volume were 266% and 121% higher for 0.25 hr relative to 6 hrs. These combined results strongly imply that longer exposure times filled the pores with PDMS. Notably, when the lower molecular weight Sigma PDMS was used with a 0.25 hr coating time, the surface area as well as the pore volume were preserved. MIL-PDMS-Dow-0.25 exhibited some pore volume reduction which may be associated with greater pore space occupation by this higher molecular weight PDMS. To further evaluate their adsorption performance corresponding to the available surface area, MIL-PDMS-0.25 and MIL-PDMS-6 samples were compared. Note that that this study only considered the impact of PDMS molecular weight on the adsorbent's pore blockage. According to a previous report, fine tuning the polymer chain architecture was a proven viable option to achieve excellent PDMS coating without compromising the adsorbent's porosity [33].

3.3. Water contact angle

The extent of hydrophobicity on the MOF's outer surface and in its internal pores was evaluated using water contact angles and a vapour adsorption-based hydrophobicity index (HI), respectively. The static contact angles reported in Table 1 were measured using sessile drop method with water, though these measurements were not possible for AC due to its granular nature and surface roughness. However, AC is well accepted to be a hydrophobic material with a high water contact angle value (120° ± 2) [45] whereas MIL-101 has a contact angle of 0° with water because of its innate hydrophilicity. After 0.25 hr coating time both the MIL-PDMS-Sigma and Dow samples, have contact angles are the same as unmodified MIL-101. This result is slightly surprising and is most likely due to incomplete external surface coverage by the PDMS coating eg patchwise coating. However, after 6 hrs of coating, the deposited PDMS resulted in an increased contact angle >130°, confirming successful external surface modification from a hydrophilic to a hydrophobic surface (Fig. S7). The influence of prolonged coating time on the sample's hydrophobicity agrees well with other reports in the literature [30,46]. Although controlling the PDMS layer thickness uniformity can certainly improve the adsorbents' surface hydrophobicity, it is considered more essential to assess the impact of the treatment on

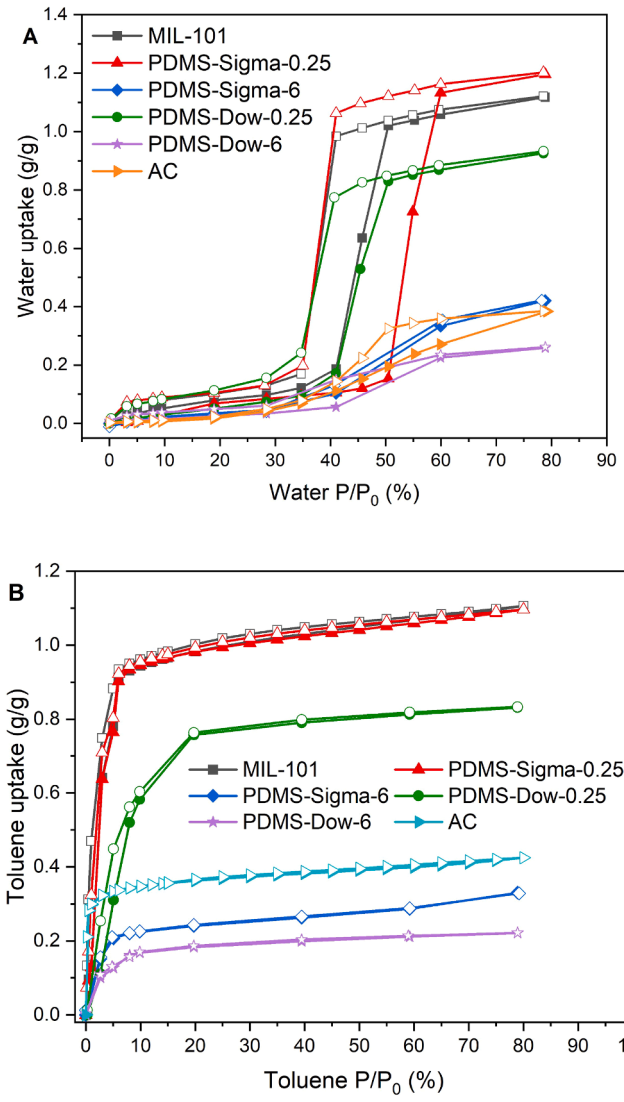

Fig. 2. Water (A) and dry toluene (B) adsorption–desorption isotherms at 25 °C. Filled symbols and empty symbols are the adsorption and desorption data points respectively.

MIL-101′s internal hydrophobicity for VOC adsorption applications.

3.4. Water adsorption isotherms

Fig. 2A shows the water adsorption and the desorption isotherms of all samples. Details on water adsorption mechanisms for MIL-101 have been reported previously in which the water molecules initially bind to the metal sites on the MOF scaffold, followed by gradual occupation of the mesopores. During this initial adsorption stage, additional water build-up leads to formation of small hydrogen-bound water clusters. Finally, the water uptake proceeds at a slower rate as the molecules transfer into the large molecular cages and the remaining inter particulate voids before reaching uptake saturation [47,48]. The water adsorption isotherm for MIL-101 displays two distinct adsorption steps; a first step at 35 to 40% water P/P_0 and a second step between 40 and 50% water P/P_0, confirming the presence of two mesoporous cages with different aperture sizes [20].

After the 0.25 hr coating time, MIL-PDMS-Sigma-0.25 exhibited no decrease in its Type-V water uptake isotherm compared with the pristine form. Even though Table 1 shows MIL-PDMS-Sigma-0.25 has a 10% higher BET surface area than the pristine MIL-101, this increase is fortuitous due to some small variations in the MOFs batches produced.

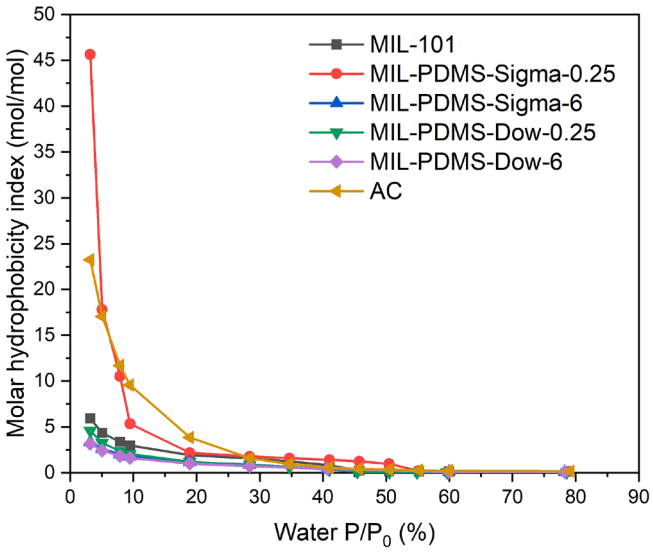

Fig. 3. Calculated molar hydrophobicity index (HI) for selected adsorbents as a function of % water P/P_0 at 25 °C.

For the 6-hr coated MIL-101 samples, the reductions in water uptake capacity correlated with their respective surface area reduction. Despite this CVD technique being commonly used [29,30,32,33,49], the risks of severe pore blockage reported here highlight the need for a careful application process to be an effective means to enhance MIL-101′s hydrophobicity. Whilst longer coating times yielded greater surface hydrophobicity, excessive duration negatively impeded pore access [30]. Both 6 hr-coated MIL-101 samples exhibited substantial pore blockage. MIL-PDMS-Dow-6 suffered the greatest porosity loss, hence its low water uptake at 80% water P/P_0.

There appears to be a divergence between a material's external surface hydrophobicity and its water adsorption isotherms. The reason is because a water contact angle measurement can only interrogate the external surface chemistry that highly depends on the surface morphology and structure (i.e., grain size and arrangement), as well as the uniformity of any surface treatments being used. On the other hand, a material's water isotherms are representative of the adsorption chemistry arising from its internal hydrophobicity. Furthermore, water contact angles on irregular surfaces, such as particulate substrates, are partially dependent on the substrate's roughness [46,50]. This behaviour is demonstrated by AC as the intrinsically hydrophobic pores resulted in a slower, gradual water uptake until it is capped by the material surface area. The 80% P/P_0 water uptake performance of the adsorbents can therefore be ranked as follows : MIL-PDMS-Dow-6 < AC < MIL-PDMS-Sigma-6 < MIL-PDMS-Dow-0.25 < MIL-101 < MIL-PDMS-Sigma-0.25

3.5. Toluene adsorption isotherms

Fig. 2B shows the amount of dry toluene adsorbed by all samples as a function of toluene % P/P_0. MIL-PDMS-Sigma-0.25 and MIL-101 have almost identical and the highest adsorption capacity at 80% toluene P/P_0; 110 wt%. This result is also 260% higher than the industrial AC. Even though these two materials have hydrophobic and hydrophilic pores respectively, toluene which has a low surface tension (28.5 mJ/m^2), will exhibit a contact angle of close to 0° for both materials. In the case of the MOF, its high surface energy will result in a contact angle of 0°, whereas for PDMS, which is swellable by toluene, will similarly exhibit a small contact angle. Thus very similar toluene isotherms, including the mesopore filling regions, are observed in Fig. 2B. Reductions in toluene adsorption for the other MIL materials generally scale with their available surface area and pore volume. For example, MIL-PDMS-Dow-6 has

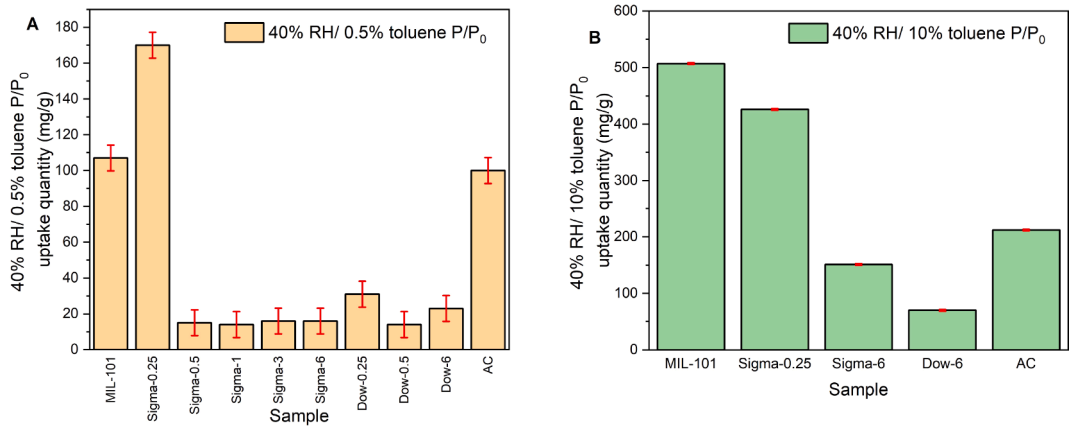

Fig. 4. Toluene uptake quantity by PDMS-coated MIL-101 samples at (A) 0.5% toluene P/P_0 and (B) 10% toluene P/P_0. All experiments were performed at 40% RH and at 25 °C.

the lowest toluene uptake, lowest surface area and lowest pore volume.

To examine the adsorption rate at low toluene P/P_0 range (<10% toluene P/P_0), the quantity of toluene uptake was plotted against the adsorption time, and the plots are shown in Fig. S8. Interestingly, AC showed faster adsorption rate in this condition which reveals the utility of AC at low toluene P/P_0 when only a single adsorbate species is present, whilst MOFs are preferred for adsorbing higher toluene quantities due to their high 80% toluene P/P_0 adsorption capacity [51].

3.6. Hydrophobicity index

Fig. 3 shows the experimentally estimated HI values as a function of humidity for all samples. Below 10% RH, the HI value of MIL-PDMS-Sigma-0.25 is between 2 and 8 times higher than MIL-101. Therefore, MIL-PDMS-Sigma-0.25 is expected to offer superior VOC capture in low RH environment. Above 10% RH, AC exhibits the highest HI values. This suggests that AC could perform better if the application involves higher humidity between 10 and 50% RH. Nevertheless, as the humidity level increases, all samples will become fully saturated with adsorbed water, eventually losing some of their capability to readily adsorb hydrophobic organic molecules [43].

3.7. Water and toluene co-adsorption experiments

The increased hydrophobicity of the mesopores in MIL-PDMS-Sigma-0.25 has a clear impact on the water mesopore filling events as shown by the isotherms in Fig. 2A. a careful examination of Fig. 2A shows that the mesopore filling by water starts at around 35 to 40% water P/P_0 for MIL-101. However, for MIL-PDMS-Sigma-0.25, the start of pore filling is delayed to between 45% – 50% P/P_0. This delay in pore filling can be directly ascribed to the change in contact angle for water condensing in these pores, and the Kelvin equation described condensation vapor pressures. In the case of the original MIL-101 surface, the contact angle between water and MIL-101 will be 0°, whilst for water on a PDMS coated surface such as a mesopore, the contact angle of about 130° would be expected. The Kelvin equation which broadly governs condensation events within pores and the vapor pressures at which these events occur, depends on the contact angle the liquid makes with the pore surface as this governs the local capillary curvature and vapour pressure. Higher liquid contact angles result in lower radii of curvature for condensing droplets in pores which results in higher vapour pressures for pore condensation to occur. For hydrophobic and hydrophilic variants of MCM-41, David et al. [52] reported an increase in pore filling humidities from 45% to 70% P/P_0 of water for 2.4 nm hydrophilic pores compared to the hydrophobic pores, for the nominally identical pore sizes. In the case of 9 nm pores the authors reported a hydrophobic MCM-41 which exhibited no pore filling below 80% P/P_0 of water adsorption or desorption. That is, whenever the humidity was under 80% P/P_0 the mesopores were effectively empty.

Co-adsorption results corresponding to 40% RH/0.5% toluene P/P_0 adsorption capacity are displayed in Fig. 4A whilst Fig. 4B shows the data at 40% RH/10% toluene P/P_0. In, Fig. 4A the PDMS coating on MIL-PDMS-Sigma-0.25 helped to achieve a 60% higher final toluene uptake level compared to the standard MIL-101; 170 and 107 mg/g respectively. AC fell slightly behind these two MOFs, adsorbing about 100 mg/g, but its pore diffusion kinetics is very slow (see Fig. 5A). It is also apparent that even for the shortest coating time, MIL-PDMS-Dow-0.25′s performance at 40% RH/0.5% toluene P/P_0 is inferior to the substantial improvement exhibited by MIL-PDMS-Sigma-0.25. For this reason, this former material was not taken forward for more detailed studies.

In Fig. 4B at 40% RH/10% toluene P/P_0, the pristine MIL-101 (507 mg/g) outperformed the MIL-PDMS-Sigma-0.25 (426 mg/g) uptake by about 19%. This result is somewhat surprising as it might have been anticipated that MIL-PDMS-Sigma-0.25, which at 40% RH has a significant amount of mesopores unoccupied, would have performed best, just as it did for 0.5% toluene P/P_0. Clearly the 20 times higher concentration of toluene of 10% P/P_0 versus 0.5% P/P_0 toluene is significant. One potential explanation for this behaviour is the stronger toluene affinity for the pristine MIL-101 adsorbent, at the much higher concentrations of 10% toluene P/P_0, highlighting the importance of chemical interactions between the adsorbate and the adsorbent. Specifically, the inherent donor–acceptor bonding and the π-π interactions taking place between the MOF ligands and the toluene molecules [53]. However, the importance of these hydrogen bonding and π-π interactions for toluene adsorption on the MIL-PDMS-Sigma-0.25 composite will be compromised by the low surface energy PDMS coating which will shield these chemical interactions, resulting in a lower toluene uptake compared to the pristine MIL-101.

The overall outstanding performance of MIL-101 and its MIL-PDMS-Sigma-0.25 variant is significantly due to the fact that MIL-101 has a high surface area and pore volume, thus providing a higher number of potential adsorption/condensation sites [54]. In practice, at a typical room's RH of 40%, MIL-101 will have significant amounts of its mesopores already filled by water, whilst for MIL-PDMS-Sigma-0.25, far fewer mesopores will be filled. So, in turn, when the MIL-101 is exposed at 40% RH and then to 0.5% P/P_0 of toluene vapor, it exhibits very limited pore filling ability to adsorb toluene on the remaining vacant sites. Whilst MIL-PDMS-Sigma-0.25 can in contrast, offer a significantly higher toluene sorption capacity at 0.5% P/P_0 as its PDMS-coated mesopores are substantially unfilled by water at 40% RH. The amount of 0.5% toluene P/P_0 adsorbed by MIL-101 as a function of % RH (0 to 80%) is reported in Fig. S9. With virtually no toluene being adsorbed above 60% RH, this observation fully supports the complete filling of the MIL-101′s mesopores with water.

Table 2
Pseudo-first order kinetics model fitted parameters of all samples.

Sample	Experimental values and their pseudo-first order model parameters									
	40% RH/0.5% toluene P/P_0					40% RH/10% toluene P/P_0				
	q_e (mg/g)	q_m (mg/g)	$k_1 \times 10^3$ (min^{-1})	$q_e.k_1$ (mg/g. min)	R^2	q_e (mg/g)	q_m (mg/g)	$k_1 \times 10^3$ (min^{-1})	$q_e.k_1$ (mg/g. min)	R^2
MIL-101	107	111	1.9	0.203	0.997	507	522	12.1	6.135	0.991
MIL-PDMS-Sigma-0.25	170	185	1.6	0.272	0.998	426	437	13.2	5.623	0.989
MIL-PDMS-Sigma-6	16	15	11.8	0.189	0.927	151	153	20	3.020	0.987
MIL-PDMS-Dow-0.25	31	31	7.8	0.242	0.989	–	–	–	–	–
MIL-PDMS-Dow-6	23	25	4.0	0.092	0.999	70	70	37.9	2.653	0.991
AC	–	–	–	–	–	212	232	9.9	2.010	0.994

Based on the $q_e.k_1$ values for 40% RH/0.5% toluene P/P_0, the increasing order of the best material is: MIL-PDMS-Dow-6 < MIL-PDMS-Sigma-6 < MIL-101 < MIL-PDMS-Dow-0.25 < MIL-PDMS-Sigma-0.25

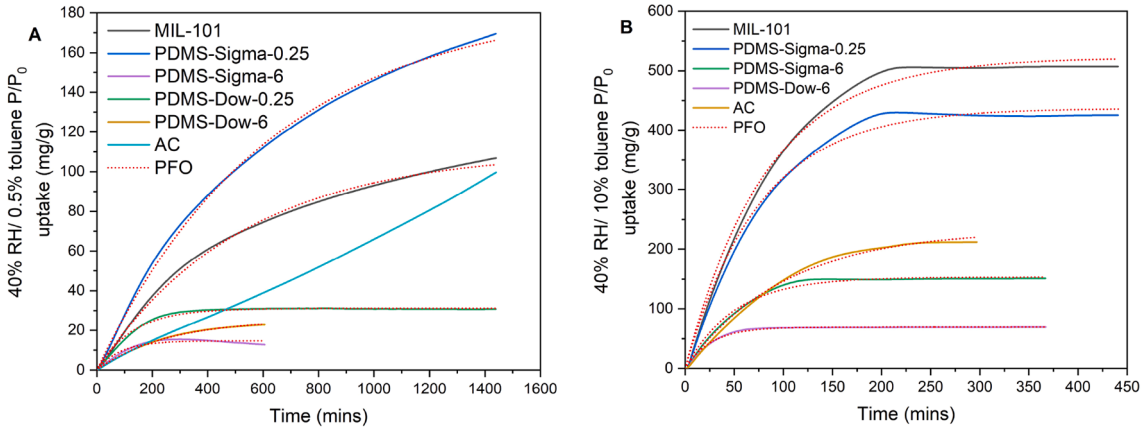

Fig. 5. Adsorption kinetics at 40% RH and at (A) 0.5% toluene P/P_0 and (B) at 10% toluene P/P_0. Solid coloured lines are the experimental data whereas the dotted red lines are the fitted values obtained from pseudo first order (PFO) model.

3.8. Kinetics modelling and analysis

Fig. 5A shows the adsorption kinetics by all modified MIL-101 samples at 40% RH with 0.5% toluene P/P_0. MIL-101, MIL-PDMS-Sigma-0.25 and MIL-PDMS-Dow-0.25 all show incredibly faster uptake rate than the very slow AC which further demonstrates the benefit of the PDMS treatment. Fig. 5B displays the adsorbents' toluene uptake kinetics at 40% RH and 10% toluene P/P_0. At both 0.5% and 10% toluene P/P_0, similar trend was observed where AC performed poorly with slower adsorption kinetics than MIL-PDMS-Sigma-0.25.

Table 2 details the calculated pseudo first order (PFO) kinetics parameters for the results in Fig. 5 (A and B). The kinetics parameters could not be calculated for AC at 0.5% toluene P/P_0 as its high micro porosity prevents it from reaching equilibrium uptake (q_e) within the specified DVS' measurement thresholds (dm/dt = 0.001 or 1440 mins, whichever comes first). The two main parameters that can be derived from the PFO model are maximum theoretical equilibrium capacity (q_m) and PFO kinetics coefficient (k_1). Ideally, for practical and industrial applications, a material should have high values in both categories, meaning it will be able to adsorb a high quantity of adsorbate at a fast rate. For a better understanding of each material's performance and a convenient ranking assortment, a new metric is proposed by taking the product of the equilibrium capacity and the PFO kinetics coefficients ($q_e.k_1$) or interchangeably termed as the aggregate adsorption rate.

Although MIL-PDMS-Dow-0.25 showed a low q_e, it has a high k_1 which makes it suitable for applications where fast adsorption is required. This data also confirms the superior performance of the MIL-PDMS-Sigma-0.25 composite over other studied materials.

At 40% RH/10% toluene P/P_0, the pristine MIL-101 has the highest $q_e.k_1$, followed by MIL-PDMS-Sigma-0.25, MIL-PDMS-Sigma-6, MIL-PDMS-Dow-6 and lastly AC. Remarkably, MIL-PDMS-Sigma-0.25 has good performance at both toluene concentrations, suggesting this material may be the right starting point for further optimization work. Compared to the MOFs, AC offers relatively modest overall performance which is only compensated for by its very low cost.

3.9. Moisture stability and reusability tests

Table S1 shows the humidity performance test results for MIL-101, MIL-PDMS-Sigma-0.25 and AC at 90% RH. This preliminary data shows that at high relative humidity, both MIL-101 materials are poor at VOC capture as their mesopore adsorption sites are still fully occupied with water molecules [55]. The hydrophobic AC, on the other hand is very selective towards toluene even after pre-exposure to 90% RH. Fig. S10 and S11 compare the amount of toluene adsorbed by the adsorbents after being subjected to 10 adsorption/desorption cycles. All materials demonstrated reliable and consistent performance across these 10 adsorption/desorption cycles.

4. Conclusions

In summary, a series of MIL-101-PDMS composites were fabricated by optimising the polymer vapour deposition time and molecular weights. Longer coating times of 6 hrs led to pore blockage as evident from the substantial decrease in the composites' surface area and pore volume. Alternatively, a 0.25 hr coating time using a lower molecular weight PDMS produced the best MIL-101 composite (MIL-PDMS-Sigma-0.25) which exhibited equivalent surface area and porosity with the unmodified MIL-101. This composite has the highest hydrophobicity index values among all samples evaluated at <10% RH. MIL-PDMS-Sigma-0.25 and MIL-101 were assessed for competitive adsorption of toluene (0.5% P/P_0 and 10% P/P_0) at 40% RH and 25 °C. At 40% RH/

0.5% toluene P/P_0 (188 ppm, concentration commonly seen in practical VOC capture applications), the composite demonstrated a 60% higher toluene uptake (170 mg/g) compared to the regular MIL-101 (107 mg/g), as well as a 34% increased aggregate adsorption rate (inclusive of both toluene uptake capacity and adsorption kinetics). The composite's superior performance at 40% RH/0.5% toluene P/P_0 could be directly attributed to the shift in the mesopore condensation/pore filling processes in its now hydrophobic mesopores. At 40% RH/10% toluene P/P_0, MIL-101 exhibited a higher uptake (507 mg/g) than the composite (426 mg/g) which highlights the importance of uncoated, native MOF framework's strong chemical interactions with toluene for these higher toluene concentrations. Additionally, this new composite demonstrated a 2.8 times higher aggregate adsorption rate than activated carbon, the industry reference material. Optimized MIL-101-PDMS composites of the type described in this work could form the basis of future adsorbent materials for the environmental capture of hydrophobic VOCs.

Declaration of Competing Interest

The authors declare that they have no known competing financial interests or personal relationships that could have appeared to influence the work reported in this paper.

Acknowledgements

The authors are grateful to Patricia Carry and Kaho Cheung for their assistance with adsorbent characterization experiments. L. H. Mohd Azmi would like to thank Yayasan Khazanah for the PhD sponsorship that made this work possible. E. Hunter-Sellars would like to thank the EPSRC Centre for Doctoral Training in Advanced Characterization of Materials (grant reference: EP/L015277/1), as well as Procter & Gamble Co., USA, for funding his work. P. Cherukupally and D. R. Williams are grateful for the Research England's Global Challenges Research Fund.

Appendix A. . Supplementary information

The following file is available free of charge.

Appendix B. Supplementary data

Supplementary data to this article can be found online at https://doi.org/10.1016/j.cej.2021.132304.

References

[1] K.W. Tham, Indoor air quality and its effects on humans—a review of challenges and developments in the last 30 years, Energy Build. 130 (2016) 637–650.
[2] B.C. McDonald, J.A. de Gouw, J.B. Gilman, S.H. Jathar, A. Akherati, C.D. Cappa, J. L. Jimenez, J. Lee-Taylor, P.L. Hayes, S.A. McKeen, Volatile chemical products emerging as largest petrochemical source of urban organic emissions, Science 359 (2018) 760–764.
[3] S.-K. Song, Z.-H. Shon, Y.-H. Kang, K.-H. Kim, S.-B. Han, M. Kang, J.-H. Bang, I. Oh, Source apportionment of VOCs and their impact on air quality and health in the megacity of Seoul, Environ. Pollut. 247 (2019) 763–774.
[4] N. Shinohara, F. Ángeles, R. Basaldud, B. Cardenas, S. Wakamatsu, Reductions in commuter exposure to volatile organic compounds in Mexico City due to the environmental program ProAire2002–2010, J. Expo. Sci. Environ. Epidemiol. 27 (3) (2017) 339–345.
[5] S. Çankaya, H. Pekey, B. Pekey, B. Özerkan Aydın, Özerkan Aydın, Volatile organic compound concentrations and their health risks in various workplace microenvironments, Hum. Ecol. Risk Assess. An Int. J. 26 (3) (2020) 822–842.
[6] X. Lu, L. Zhang, X. Wang, M. Gao, K. Li, Y. Zhang, X. Yue, Y. Zhang, Rapid increases in warm-season surface ozone and resulting health impact in China since, Environ Sci. Technol. Lett. 7 (2020) (2013) 240–247.
[7] Wolfgang Rosenberger, Effect of charcoal equipped HEPA filters on cabin air quality in aircraft. a case study including smell event related in-flight measurements, Build. Environ. 143 (2018) 358–365.
[8] K.J. Heo, J.W. Noh, B.U. Lee, Y. Kim, J.H. Jung, Comparison of filtration performance of commercially available automotive cabin air filters against various airborne pollutants, Build. Environ. 161 (2019), 106272.
[9] Lin-Hua Xie, Xiao-Min Liu, Tao He, Jian-Rong Li, Metal-organic frameworks for the capture of trace aromatic volatile organic compounds, Chem. 4 (8) (2018) 1911–1927.
[10] Christina V. McGuire, Ross S. Forgan, The surface chemistry of metal–organic frameworks, Chem. Commun. 51 (25) (2015) 5199–5217.
[11] W. Wang, X. Mi, H. Shi, X. Zhang, Z. Zhou, C. Li, D. Zhu, Adsorption behaviour and mechanism of the PFOS substitute OBS (sodium p-perfluorous nonenoxybenzene sulfonate) on activated carbon, R. Soc. Open Sci. 6 (2019), 191069.
[12] Xiuquan Li, Li Zhang, Zhongqing Yang, Peng Wang, Yunfei Yan, Jingyu Ran, Adsorption materials for volatile organic compounds (VOCs) and the key factors for VOCs adsorption process: a review, Sep. Purif. Technol. 235 (2020) 116213, https://doi.org/10.1016/j.seppur.2019.116213.
[13] Lin-Hua Xie, Ming-Ming Xu, Xiao-Min Liu, Min-Jian Zhao, Jian-Rong Li, Hydrophobic metal-organic frameworks: assessment, construction, and diverse applications, Adv. Sci. 7 (4) (2020) 1901758, https://doi.org/10.1002/advs.v7.410.1002/advs.201901758.
[14] Chan-Yuan Huang, Ming Song, Zhi-Yuan Gu, He-Fang Wang, Xiu-Ping Yan, Probing the adsorption characteristic of metal-organic framework MIL-101 for volatile organic compounds by quartz crystal microbalance, Environ. Sci. Technol. 45 (10) (2011) 4490–4496, https://doi.org/10.1021/es200256q.
[15] Zhenxia Zhao, Xuemei Li, Zhong Li, Adsorption equilibrium and kinetics of p-xylene on chromium-based metal organic framework MIL-101, Chem. Eng. J. 173 (1) (2011) 150–157.
[16] Shikai Xian, Ying Yu, Jing Xiao, Zhijuan Zhang, Qibin Xia, Haihui Wang, Zhong Li, Competitive adsorption of water vapor with VOCs dichloroethane, ethyl acetate and benzene on MIL-101 (Cr) in humid atmosphere, RSC Adv. 5 (3) (2015) 1827–1834.
[17] Xingjie Wang, Chen Ma, Jing Xiao, Qibin Xia, Junliang Wu, Zhong Li, Benzene/toluene/water vapor adsorption and selectivity of novel C-PDA adsorbents with high uptakes of benzene and toluene, Chem. Eng. J. 335 (2018) 970–978.
[18] Botao Liu, Kumar Vikrant, Ki-Hyun Kim, Vanish Kumar, Suresh Kumar Kailasa, Critical role of water stability in metal–organic frameworks and advanced modification strategies for the extension of their applicability, Environ. Sci. Nano. 7 (5) (2020) 1319–1347.
[19] Nakeun Ko, Jisu Hong, Siyoung Sung, Kyle E. Cordova, Hye Jeong Park, Jin Kuk Yang, Jaheon Kim, A significant enhancement of water vapour uptake at low pressure by amine-functionalization of UiO-67, Dalt. Trans. 44 (5) (2015) 2047–2051.
[20] Kosuke Yanagita, Junho Hwang, Jubair A. Shamim, Wei-Lun Hsu, Ryotaro Matsuda, Akira Endo, Jean-Jacques Delaunay, Hirofumi Daiguji, Kinetics of water vapor adsorption and desorption in MIL-101 metal-organic frameworks, J. Phys. Chem. C. 123 (1) (2019) 387–398, https://doi.org/10.1021/acs.jpcc.8b08211.
[21] Chi Yang, Ushasree Kaipa, Qian Zhang Mather, Xiaoping Wang, Vladimir Nesterov, Augustin F. Venero, Mohammad A. Omary, Fluorous metal-organic frameworks with superior adsorption and hydrophobic properties toward oil spill cleanup and hydrocarbon storage, J. Am. Chem. Soc. 133 (45) (2011) 18094–18097, https://doi.org/10.1021/ja208408n.
[22] M. Zhu, P. Hu, Z. Tong, Z. Zhao, Z. Zhao, Enhanced hydrophobic MIL(Cr) metal-organic framework with high capacity and selectivity for benzene VOCs capture from high humid air, Chem. Eng. J. 313 (2017) 1122–1131, https://doi.org/10.1016/j.cej.2016.11.008.
[23] Prasanth Karikkethu Prabhakaran, Johnny Deschamps, Doping activated carbon incorporated composite MIL-101 using lithium: impact on hydrogen uptake, J. Mater. Chem. A. 3 (13) (2015) 7014–7021, https://doi.org/10.1039/C4TA07197B.
[24] M.L. Díaz-Ramírez, E. Sánchez-González, J.R. Álvarez, G.A. González-Martínez, S. Horike, K. Kadota, K. Sumida, E. González-Zamora, M.-A. Springuel-Huet, A. Gutiérrez-Alejandre, Partially fluorinated MIL-101 (Cr): from a miniscule structure modification to a huge chemical environment transformation inspected by 129 Xe NMR, J. Mater. Chem. A. 7 (2019) 15101–15112.
[25] E. Martínez-Ahumada, M.L. Díaz-Ramírez, H.A. Lara-García, D.R. Williams, V. Martis, V. Jancik, E. Lima, I.A. Ibarra, High and reversible SO_2 capture by a chemically stable Cr (iii)-based MOF, J. Mater. Chem. A. 8 (2020) 11515–11520.
[26] Fanyu Zhang, Xinxin Sang, Xiuniang Tan, Chengcheng Liu, Jianling Zhang, Tian Luo, Lifei Liu, Buxing Han, Guanying Yang, Bernard P. Binks, Converting metal-organic framework particles from hydrophilic to hydrophobic by an interfacial assembling route, Langmuir. 33 (43) (2017) 12427–12433, https://doi.org/10.1021/acs.langmuir.7b02365.
[27] Q. Sun, H. He, W.-Y. Gao, B. Aguila, L. Wojtas, Z. Dai, J. Li, Y.-S. Chen, F.-S. Xiao, S. Ma, Imparting amphiphobicity on single-crystalline porous materials, Nat. Commun. 7 (2016) 13300.
[28] Peter Thurgood, Sara Baratchi, Crispin Szydzik, Arnan Mitchell, Khashayar Khoshmanesh, Porous PDMS structures for the storage and release of aqueous solutions into fluidic environments, Lab Chip. 17 (14) (2017) 2517–2527.
[29] Wang Zhang, Yingli Hu, Jin Ge, Hai-Long Jiang, Shu-Hong Yu, A facile and general coating approach to moisture/water-resistant metal-organic frameworks with intact porosity, J. Am. Chem. Soc. 136 (49) (2014) 16978–16981, https://doi.org/10.1021/ja509960n.
[30] G. Huang, Q. Yang, Q. Xu, S. Yu, H. Jiang, Polydimethylsiloxane coating for a palladium/MOF composite: highly improved catalytic performance by surface hydrophobization, Angew. Chemie Int. Ed. 55 (2016) 7379–7383.
[31] Xiao-Yu Xu, Bing Yan, Nanoscale LnMOF-functionalized nonwoven fibers protected by a polydimethylsiloxane coating layer as a highly sensitive ratiometric oxygen sensor, J. Mater. Chem. C. 4 (36) (2016) 8514–8521.

[32] Minjung Kang, Jeong Eun Kim, Dong Won Kang, Hwa Young Lee, Dohyun Moon, Chang Seop Hong, A diamine-grafted metal-organic framework with outstanding CO2 capture properties and a facile coating approach for imparting exceptional moisture stability, J. Mater. Chem. A. 7 (14) (2019) 8177–8183, https://doi.org/10.1039/C8TA07965J.
[33] Sanfeng He, Lihan Chen, Jing Cui, Biao Yuan, Hongliang Wang, Fang Wang, Yi Yu, Yongjin Lee, Tao Li, General way to construct micro- and mesoporous metal–organic framework-based porous liquids, J. Am. Chem. Soc. 141 (50) (2019) 19708–19714, https://doi.org/10.1021/jacs.9b08458.
[34] X. Li, L. Zhang, Z. Yang, Z. He, P. Wang, Y. Yan, J. Ran, Hydrophobic modified activated carbon using PDMS for the adsorption of VOCs in humid condition, Sep. Purif. Technol. 239 (2020) 1–10.
[35] United States Department of Labor, Substance Safety Data Sheet, Benzene, 1910.1028 App A Occup. Saf. Heal. Stand. (2021). https://www.osha.gov/laws-regs/regulations/standardnumber/1910/1910.1028AppA#:~:text=1.,for any 15-minute period. (accessed May 26, 2021).
[36] United States Department of Labor, Toluene Occupational Exposure Limits, Occup. Saf. Heal, Adm, 2021 https://www.osha.gov/toluene/occupational-exposure-limits (accessed May 5, 2021).
[37] Luqman Hakim Mohd Azmi, Daryl Williams, Bradley P. Ladewig, Can metal organic frameworks outperform adsorptive removal of harmful phenolic compound 2-chlorophenol by activated carbon? Chem. Eng. Res. Des. 158 (2020) 102–113.
[38] Clearco, Properties of Polydimethylsiloxane Fluids, 2015. www.clearcoproducts.com.
[39] E. Hunter-Sellars, P.A. Saenz-Cavazos, A.R. Houghton, S.R. McIntyre, I.P. Parkin, D.R. Williams, Sol-gel synthesis of high-density zeolitic imidazolate framework monoliths via ligand assisted methods: exceptional porosity, hydrophobicity, and applications in vapor adsorption, Adv. Funct. Mater. 31 (2021) 2008357.
[40] Istvan Halasz, Mukesh Agarwal, Bonnie Marcus, William E. Cormier, Molecular spectra and polarity sieving of aluminum deficient hydrophobic HY zeolites, Microporous Mesoporous Mater. 84 (1-3) (2005) 318–331.
[41] Biswa Nath Bhadra, Kyung Ho Cho, Nazmul Abedin Khan, Do-Young Hong, Sung Hwa Jhung, Liquid-phase adsorption of aromatics over a metal-organic framework and activated carbon: effects of hydrophobicity/hydrophilicity of adsorbents and solvent polarity, J. Phys. Chem. C. 119 (47) (2015) 26620–26627, https://doi.org/10.1021/acs.jpcc.5b09298.
[42] Arjan Giaya, Robert W Thompson, Raymond Denkewicz Jr, Liquid and vapor phase adsorption of chlorinated volatile organic compounds on hydrophobic molecular sieves, Microporous Mesoporous Mater. 40 (1-3) (2000) 205–218.
[43] Elwin Hunter-Sellars, J.J. Tee, Ivan P. Parkin, Daryl R. Williams, Adsorption of volatile organic compounds by industrial porous materials: impact of relative humidity, Microporous Mesoporous Mater. 298 (2020) 110090, https://doi.org/10.1016/j.micromeso.2020.110090.
[44] C. Qin, G. Wen, X. Wang, L. Song, X. Huang, Ultra-long Sialon nanobelts: large-scale synthesis via a pressure enhanced CVD process and photoluminescence characteristics, J. Mater. Chem. 21 (2011) 5985–5991.
[45] Han-Bing Liu, Bing Yang, Nan-Dong Xue, Enhanced adsorption of benzene vapor on granular activated carbon under humid conditions due to shifts in hydrophobicity and total micropore volume, J. Hazard. Mater. 318 (2016) 425–432.
[46] Z. Gao, G. Song, X. Zhang, Q. Li, S. Yang, T. Wang, Y. Li, L. Zhang, L. Guo, Y. Fu, A facile PDMS coating approach to room-temperature gas sensors with high humidity resistance and long-term stability, Sensors Actuators B Chem. 325 (2020), 128810.
[47] Pia Küsgens, Marcus Rose, Irena Senkovska, Heidrun Fröde, Antje Henschel, Sven Siegle, Stefan Kaskel, Characterization of metal-organic frameworks by water adsorption, Microporous Mesoporous Mater. 120 (3) (2009) 325–330, https://doi.org/10.1016/j.micromeso.2008.11.020.
[48] Nakeun Ko, Pan Gyu Choi, Jisu Hong, Miso Yeo, Siyoung Sung, Kyle E. Cordova, Hye Jeong Park, Jin Kuk Yang, Jaheon Kim, Tailoring the water adsorption properties of MIL-101 metal–organic frameworks by partial functionalization, J. Mater. Chem. A. 3 (5) (2015) 2057–2064.
[49] Xianming Zheng, Shuai Liu, Sadia Rehman, Zehui Li, Pengyi Zhang, Highly improved adsorption performance of metal-organic frameworks CAU-1 for trace toluene in humid air via sequential internal and external surface modification, Chem. Eng. J. 389 (2020) 123424, https://doi.org/10.1016/j.cej.2019.123424.
[50] K. Jayaramulu, F. Geyer, A. Schneemann, Š. Kment, M. Otyepka, R. Zboril, D. Vollmer, R.A. Fischer, Hydrophobic metal-organic frameworks, Adv. Mater. 31 (2019) 1–31, https://doi.org/10.1002/adma.201900820.
[51] K.-H. Kim, J.E. Szulejko, N. Raza, V. Kumar, K. Vikrant, D.C.W. Tsang, N.S. Bolan, Y.S. Ok, A. Khan, Identifying the best materials for the removal of airborne toluene based on performance metrics-a critical review, J. Clean. Prod. 241 (2019), 118408.
[52] Robert O. David, Jonas Fahrni, Claudia Marcolli, Fabian Mahrt, Dominik Brühwiler, Zamin A. Kanji, The role of contact angle and pore width on pore condensation and freezing, Atmos. Chem. Phys. 20 (15) (2020) 9419–9440.
[53] Yong-Zhi Li, Gang-Ding Wang, Wen-Juan Shi, Lei Hou, Yao-Yu Wang, Zhonghua Zhu, Efficient C2Hn hydrocarbons and VOC adsorption and separation in an MOF with lewis basic and acidic decorated active sites, ACS Appl. Mater. Interfaces. 12 (37) (2020) 41785–41793.
[54] Kun Yang, Qian Sun, Feng Xue, Daohui Lin, Adsorption of volatile organic compounds by metal–organic frameworks MIL-101: influence of molecular size and shape, J. Hazard. Mater. 195 (2011) 124–131.
[55] B. Liu, S.A. Younis, K.-H. Kim, The dynamic competition in adsorption between gaseous benzene and moisture on metal-organic frameworks across their varying concentration levels, Chem. Eng. J. 421 (2021), 127813.